

Binary Blends of Diblock Copolymers: An Effective Route to Novel Bicontinuous Phases

Chi To Lai* and An-Chang Shi*

*Department of Physics & Astronomy, McMaster University, 1280 Main St. W, Hamilton, Ontario
L8S 4M1, Canada*

E-mail: laic13@mcmaster.ca; shi@mcmaster.ca

Abstract

The formation of various bicontinuous phases from binary blends of linear AB diblock copolymers (DBCPs) is studied using the polymeric self-consistent field theory. The theoretical study predicts that the double-diamond and the “plumber’s nightmare” phases, which are metastable for neat diblock copolymers, could be stabilized in block copolymers with designed dispersity, namely, binary blends composed of a gyroid-forming DBCP and a homopolymer-like DBCP. The spatial distribution of different monomers reveals that these two types of DBCPs are segregated such that the homopolymer-like component is localized at the nodes to relieve the packing frustration. Simultaneously, the presence of a local segregation of the two DBCPs on the AB interface regulates the interfacial curvature. These two mechanisms could act in tandem for homopolymer-like diblock copolymers with proper compositions, resulting in larger stability regions for the novel bicontinuous phases.

Introduction

The most distinguishing property of block copolymers is their ability to self-assemble into periodically ordered structures with periods on the order of 10-100 nm¹. In the simplest case of linear AB diblock copolymers, the morphology of the self-assembled structure could be systematically regulated by varying a small number of parameters. Two of these parameters are the volume fraction of the A-blocks, f_A , and the segregation strength χN , where χ is the Flory-Huggins parameter quantifying the immiscibility of the two unlike monomers and N denotes the total polymer length¹. Recently, it has also been recognized that the conformational asymmetry of block copolymers could play an important role in stabilizing complex spherical packing phases². Starting from symmetric diblock copolymers with $f_A = 0.5$, the ordered phases of the system follow a generic transition sequence of lamellar (L) \rightarrow cylindrical (C) \rightarrow bicontinuous (G) \rightarrow spherical (S) phases as the DBCPs become more asymmetric¹. Among the various ordered phases of block copolymers, the bicontinuous phases are of particular interest due to their intricate structures and their potential applications in the production of highly-porous materials³, materials with low refractive

index⁴, high-conductivity nanoparticles⁵, dye-sensitive solar cells⁶, and 3D photonic crystals⁷. Therefore, it is desirable to search for polymeric systems that could form various bicontinuous phases in a large phase space.

It is worthwhile to first briefly review the discovery of the bicontinuous phases self-assembled from block copolymers. The first report of a bicontinuous structure in AB-type block copolymers, initially designated as the double-diamond (DD) phase, was made in 1986 for poly-(styrene-*b*-isoprene) (SI) star copolymers^{8,9}. A year later, Hashimoto *et al.*¹⁰ observed a four-branched tetrapod-network structure in linear SI diblock copolymers, which was regarded as an example of the double diamond structure. In 1994, Hajduk *et al.* reported the formation of the double gyroid (G) phase in star copolymers¹¹ and in linear diblock copolymers¹². In these two studies, the authors pointed out that the bicontinuous structures observed in previous reports^{8,9} would be more compatible with the double gyroid phase. At the same time, Schulz *et al.*¹³ also observed the double gyroid phase in poly(isoprene-*b*-2-vinylpyridine). Shortly after, a self-consistent field theory calculation carried out by Matsen and Schick¹⁴ predicted that the G phase has lower free energy than that of the DD phase, thus confirming the designation of Hajduk *et al.* and Schulz *et al.*. It is now generally accepted the only bicontinuous structure accessible in monodisperse melts of linear AB diblock copolymers is the double gyroid phase¹⁵.

There exist a number of bicontinuous networked structures, consisting of two interweaving networks composed of the minority-block monomers embedded in a matrix of the majority block^{15,16}. The networks could be viewed as struts or connectors joining together at different nodes. The number of struts meeting at a node depends on the particular structure. For the double gyroid ($Ia\bar{3}d$), the double diamond ($Pn\bar{3}m$), and the plumber's nightmare (P) ($Im\bar{3}m$) phases, the number of struts per node is 3, 4, and 6, respectively. In order to minimize the surface area of the AB interface under the constant-volume constraint, the formation of a constant-mean-curvature structure is preferred¹⁷. For the bicontinuous phases, this leads the nodes becoming thicker or bulkier than the connectors, with the disparity in size increasing with the number of struts per nodes¹⁶. On the other hand, in order to maintain a uniform monomer density, polymers must stretch excessively to

fill the space at the center of the nodes^{17,18}. The competition of these two opposing trends results in packing frustration in the system. It is argued that the stability of the double gyroid phase in monodisperse diblock copolymers originates from the fact that the thickness difference between the nodes and struts is the smallest in the double gyroid structure, thus resulting in the least packing frustration¹⁷.

One way to alleviate the packing frustration at the nodes is to employ polymeric systems with designed dispersity distributions. It is well known that dispersity of block copolymers could be used to regulate their phase behaviour^{19–22}. The simplest disperse distribution is bidisperse systems, *viz.* binary blends, composed of mixtures of two types of polymers, which exhibit rich phase behaviour and offer opportunities to form desirable structures²³. For the case of bicontinuous phases, Matsen showed theoretically that the double diamond phase could be accessed in homopolymer-diblock copolymer (H+DBCP) blends²⁴. Specifically, his self-consistent field theory (SCFT) calculations demonstrated that the added homopolymers localize at the centers of the nodes, which reduces the need for the diblock copolymers to stretch excessively to fill the space, thus relieving packing frustration. The approach of introducing space-fillers was further pursued by Escobedo and coworkers using a number of theoretical techniques^{25–28}. In a Monte Carlo simulation study, Martínez-Veracoechea and Escobedo²⁵ considered selective solvents particles in addition to homopolymers as the additive component. The solvent particles were found to be distributed uniformly throughout the minority domain, and therefore, failed to reduce the packing frustration that is necessary to stabilize the double diamond, or plumber’s nightmare phases. Using SCFT, Martínez-Veracoechea and Escobedo²⁷ further demonstrated that both the blend composition or the homopolymer length could be tuned to stabilize the plumber’s nightmare phase in H+DBCP blends. A subsequent molecular dynamics study²⁸ yielded information on the chain conformations within the bicontinuous structures, which provided direct evidence that the addition of homopolymers alleviates the packing frustration occurring at the nodes. Experimentally, Takagi *et al.*²⁹ probed the phase behaviour of binary blends of SI diblock copolymers and polyisoprene homopolymers using small angle x-ray scattering. They observed the formation of the

double diamond phase, and moreover found that the order-order transition between the DD, and G phases was thermodynamically reversible. Most recently, Takagi *et al.*³⁰ demonstrated that the double diamond phase can be accessed in ternary blends of SI diblock copolymers at specific blend compositions.

To the best of our knowledge, existing theoretical studies examining the formation of bicontinuous phases in diblock copolymer blends have either considered homopolymers or solvent particles as space-filling additives. One limitation of using homopolymers is that macrophase separation occurs between the homopolymer-rich disordered phase and the adjacent bicontinuous phase at relatively low homopolymer concentrations, resulting in a small range of blend compositions over which the double diamond or plumber's nightmare phases could be formed. A possible strategy to circumvent macrophase separation is to use a polydisperse diblock copolymers in which the long and short chains could segregate to relieve the packing frustration. In this paper, we examine a bidisperse system composed of two types of AB diblock copolymers, namely a gyroid-forming diblock copolymer and a homopolymer-like diblock copolymer, where the A-blocks are taken as the network-forming component. The homopolymer-like AB diblock copolymer has an A-block that is much longer than its B-block. We employ the polymeric SCFT to construct the phase diagrams of the system. The effects of the blend composition and the volume fraction of the diblock copolymers are examined. We find that both the double diamond and plumber's nightmare phases could emerge as stable phases when the total length of the homopolymer-like component becomes sufficiently long. Moreover, the range of blend compositions over which the double diamond or plumber's nightmare phases occurs is found to be larger than that of the equivalent H+DBCP blends. By examining the spatial distribution of the polymeric species within the self-assembled structures, we find evidence that the homopolymer-like copolymers not only act as a space-filler that relieves packing frustration, but also act as co-surfactants resulting in favourable changes to the AB-interfacial curvature. The combination of these two effects results in the larger stable regions of the various bicontinuous phases.

Theoretical Model

We consider a binary mixture of diblock copolymers, $(AB)_1$ and $(AB)_2$, in a volume V . The length of the A-block, and the total length of the copolymers are given by $N_{A,c}$, and N_c , respectively with the index $c = 1$ or 2 labeling the type of diblock copolymers. The melt is assumed to be incompressible. We also assume for simplicity that the A-, and B-monomer volumes, as well as their Kuhn lengths are equal, *i.e.* $v_A = v_B$, and $b_A = b_B$. The polymer chains are modeled as Gaussian chains³¹.

Information about the thermodynamics of the system is contained in the partition function, which can be expressed as a functional integral over all chain conformations. Alternatively, the partition function can be expressed in the grand canonical ensemble as a functional integral over the monomer volume fractions $\phi_\gamma(\mathbf{r})$ and auxiliary fields $\omega_\gamma(\mathbf{r})$ as,

$$Z = \int \mathcal{D}\phi_A(\mathbf{r}) \int \mathcal{D}\phi_B(\mathbf{r}) \int \mathcal{D}\omega_A(\mathbf{r}) \int \mathcal{D}\omega_B(\mathbf{r}) \int \mathcal{D}\Xi(\mathbf{r}) \times \exp \{ -\beta G[\phi_A(\mathbf{r}), \omega_A(\mathbf{r}), \phi_B(\mathbf{r}), \omega_B(\mathbf{r}), \Xi(\mathbf{r})] \}, \quad (1)$$

where $G = G[\phi_A(\mathbf{r}), \omega_A(\mathbf{r}), \phi_B(\mathbf{r}), \omega_B(\mathbf{r}), \Xi(\mathbf{r})]$ is the free energy functional given in units of $k_B T$,^{31,32}

$$\frac{G}{\rho_0 V} = \frac{1}{V} \left\{ \int d\mathbf{r} \chi \phi_A(\mathbf{r}) \phi_B(\mathbf{r}) - \sum_{\gamma=A,B} \omega_\gamma(\mathbf{r}) \phi_\gamma(\mathbf{r}) - \Xi(\mathbf{r}) [1 - \phi_A(\mathbf{r}) - \phi_B(\mathbf{r})] \right\} - \sum_{c=1}^2 e^{\mu_c} Q_c. \quad (2)$$

Here, the index γ runs over the monomer types (*i.e.* $\gamma = A, B$), and μ_c is the chemical potential of c -type polymers in units of $k_B T$. Due to the incompressibility condition, the two chemical potentials are not independent. We can therefore set one of the chemical potentials to a convenient reference value, and vary the other in order to adjust the blend composition³³. Moreover, we have introduced a Lagrange multiplier $\Xi(\mathbf{r})$ to enforce the incompressibility condition. The single-chain partition

function for c -type polymers is defined by,

$$Q_c = \frac{1}{V} \int d\mathbf{r} q_c(\mathbf{r}, N_c), \quad (3)$$

where $q_c(\mathbf{r}, N_c)$ is the forward end-integrated propagator obeying the modified diffusion equation,

$$\frac{\partial q_c(\mathbf{r}, s)}{\partial s} = \nabla^2 q_c(\mathbf{r}, s) - \omega_c(\mathbf{r}, s) q_c(\mathbf{r}, s), \quad (4)$$

$$\omega_c(\mathbf{r}, s) = \begin{cases} \omega_A(\mathbf{r}) & 0 \leq s \leq N_{A,c} \\ \omega_B(\mathbf{r}) & N_{A,c} \leq s \leq N_c \end{cases}, \quad (5)$$

subject to the initial condition $q_c(\mathbf{r}, 0) = 1$.

In order to evaluate the free energy of the system, we apply the mean-field approximation^{31,32}, which amounts to minimizing the free energy density functional with respect the monomer concentrations, the auxiliary fields, and the Lagrange multipliers. The mean-field approximation leads to a set of SCFT equations whose solutions corresponding to various ordered phases of block copolymers could be obtained using available numerical methods. It is also noted that the mean-field approximation also ignores correlations between fluctuations that could be important near the critical point of the system³¹. The minimization procedure leads a set of self-consistent equations. Performing the minimization with respect to the concentrations gives,

$$\omega_A(\mathbf{r}) = \chi \phi_B(\mathbf{r}) + \Xi(\mathbf{r}), \quad \omega_B(\mathbf{r}) = \chi \phi_A(\mathbf{r}) + \Xi(\mathbf{r}). \quad (6)$$

The incompressibility condition is recovered when minimizing with respect to $\Xi(\mathbf{r})$,

$$\phi_A(\mathbf{r}) + \phi_B(\mathbf{r}) = 1. \quad (7)$$

We can lastly determine the equilibrium monomer volume fractions by extremizing with respect

to the auxiliary fields, which yields,

$$\begin{aligned}\phi_A(\mathbf{r}) &= \sum_{i=1}^2 e^{\mu_c} \int_0^{N_{A,c}} ds q_c(\mathbf{r}, s) q_c^\dagger(\mathbf{r}, N_c - s), \\ \phi_B(\mathbf{r}) &= \sum_{i=1}^2 e^{\mu_c} \int_{N_{A,c}}^{N_c} ds q_c(\mathbf{r}, s) q_c^\dagger(\mathbf{r}, N_c - s),\end{aligned}\tag{8}$$

where $q_c^\dagger(\mathbf{r}, s)$ is the backward end-integrated propagator that satisfies a similar diffusion equation to Eq. (4),

$$\frac{\partial q_c^\dagger(\mathbf{r}, s)}{\partial s} = \nabla^2 q_c^\dagger(\mathbf{r}, s) - \omega_c^\dagger(\mathbf{r}, s) q_c(\mathbf{r}, s),\tag{9}$$

$$\omega_c^\dagger(\mathbf{r}, s) = \begin{cases} \omega_B(\mathbf{r}) & 0 \leq s \leq N_c - N_{A,c} \\ \omega_A(\mathbf{r}) & N_c - N_{A,c} < s \leq N_c \end{cases},\tag{10}$$

once more subject to the initial condition, $q_c^\dagger(\mathbf{r}, 0) = 1$.

There are multiple solutions to the self-consistent equations, corresponding to different possible phases of the system. Spatially-varying solutions correspond to the ordered structures, while a constant solution that can always be found represents the homogeneous disordered phase. Barring a few exceptions, solutions to the SCFT equations are generally determined using numerical methods. For an ordered phase, numerically solving the SCFT equations could be conveniently done within one unit cell of the structure. However, the resulting free energy will be dependent on the unit-cell parameters, and therefore, minimization over these parameters must also be performed. We employ Anderson mixing³⁴ to iteratively solve the SCFT equations, and gradient descent to find the optimal lattice parameters. The pseudospectral method^{35,36} is employed within each iteration to solve the diffusion equations, Eqs. (4), and (9). Calculations proceed until the maximum difference in the free energy density between three consecutive iterations is less than 10^{-6} . The equilibrium phase is then determined by a comparison of the free energies of the candidate structures. In this study, we consider the disordered (DIS), lamellar (L), and hexagonally-packed cylindrical (C) phases alongside the bicontinuous double gyroid (G), double diamond (DD), and plumber's nightmare (P) phases as the candidate structures. In the grand canonical ensemble for-

mulation of the theory, the chemical potential μ_2 is the control parameter. The chemical potentials can be related to the average volume fractions of either polymer types via,

$$\bar{\phi}_2 = e^{\mu_2} N_2 Q_2 = 1 - \bar{\phi}_1 = 1 - N_1 Q_1, \quad (11)$$

where the last two equalities were obtained from the incompressibility condition, $\bar{\phi}_1 + \bar{\phi}_2 = 1$, and the condition $\mu_1 = 0$.

Results and Discussions

In this section, we present our results on the phase behaviour of binary blends composed of gyroid-forming diblock copolymers and homopolymer-like copolymers. We use the subscripts G and HL to denote quantities associated with the gyroid-forming and homopolymer-like copolymers, respectively. The relative lengths of the two polymers are characterized by the parameter $\alpha = N_{\text{HL}}/N_{\text{G}}$. For the homopolymer-like copolymer, we set its A-block volume fraction to be $f_{\text{A,HL}} = N_{\text{A,HL}}/N_{\text{HL}} = 0.95$.

We first examine the effect of the blend composition ($\bar{\phi}_{\text{HL}}$) and the ratio of total polymer lengths (α) on the phase behaviour of the blends. Figure. 1 shows the phase diagram in the $\bar{\phi}_{\text{HL}}-\alpha$ plane for the case of $f_{\text{A,G}} = 0.33$ and $\chi N_{\text{G}} = 25$. In all the phase diagrams, the single-phase regions are labeled their phases, whereas the two-phase coexistence regions are left unlabeled. As shown in Figure 1, the G phase is the only equilibrium structure when $\bar{\phi}_{\text{HL}} = 0$ as expected. A new phase emerges once a sufficient amount of homopolymer-like copolymers are added to the system. For $1.4 \leq \alpha \leq 1.45$, the G phase is replaced by the DD phase, whereas for $\alpha \geq 1.45$, hexagonally-packed cylinders are predicted to appear first. The cylindrical phase subsequently transforms to the DD phase upon further increasing $\bar{\phi}_{\text{HL}}$ except near the largest values of α shown. In all cases, the equilibrium morphology reenters to the double gyroid phase once the additive concentration exceeds $\bar{\phi}_{\text{HL}} = 0.25$.

There are a number of differences in the phase behaviours of binary blends of diblock copoly-

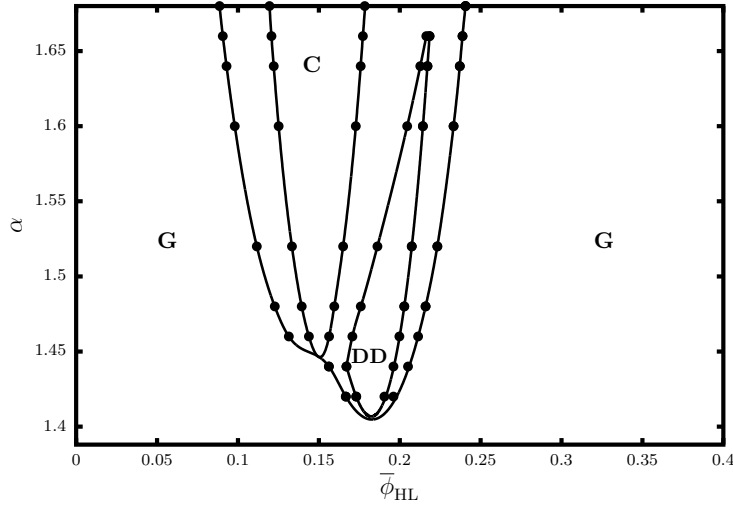


Figure 1: Phase diagram of the binary mixture with $\chi N_G = 25$, $f_{A,G} = 0.33$, and $f_{A,HL} = 0.95$ in the $\bar{\phi}_{HL}$ - α plane. The labels, C, G, and DD, correspond to the hexagonal, double gyroid, and double diamond phases, respectively. Unlabeled areas denote regions of phase co-existence between the two bordering phases. The circular points represent the numerically computed data, while the lines serve as guide for the eyes.

mers mixed with homopolymers (AB/A) or homopolymer-like diblock copolymers (AB/AB). First of all, the emergence of the DD phase in H+DBCP blends has been predicted to occur for the cases where the homopolymers are shorter than the G-forming diblock copolymers ($\alpha < 1$)^{25–28}. On the other hand, it is clear from the Figure 1 that the DD phase could only be accessed when the homopolymer-like copolymers are longer than the G-forming diblock copolymers ($\alpha > 1$). Secondly, the DD or P phase in the AB/A system is always found at blend compositions where the system is close to becoming saturated with homopolymers, such that further increasing the homopolymer concentration would cause macrophase separation between the H-rich disordered phase and the ordered DD or P phase. On the other hand, the AB/AB system could continue to accept additional homopolymer-like copolymers after reaching the DD phase, eventually reentering to the double gyroid phase. It is worthwhile to note that the subsequent re-entrance to the double gyroid phase, as well as the phase transition sequence $G \leftrightarrow DD \leftrightarrow G$ have been observed experimentally in ternary mixtures of simple SI diblock copolymers³⁰.

We next examine the effects of the composition of the gyroid-forming diblock copolymers. Figure (2) presents phase diagrams in the $\bar{\phi}_{HL}$ - α plane with $\chi N_G = 25$ for two gyroid-forming

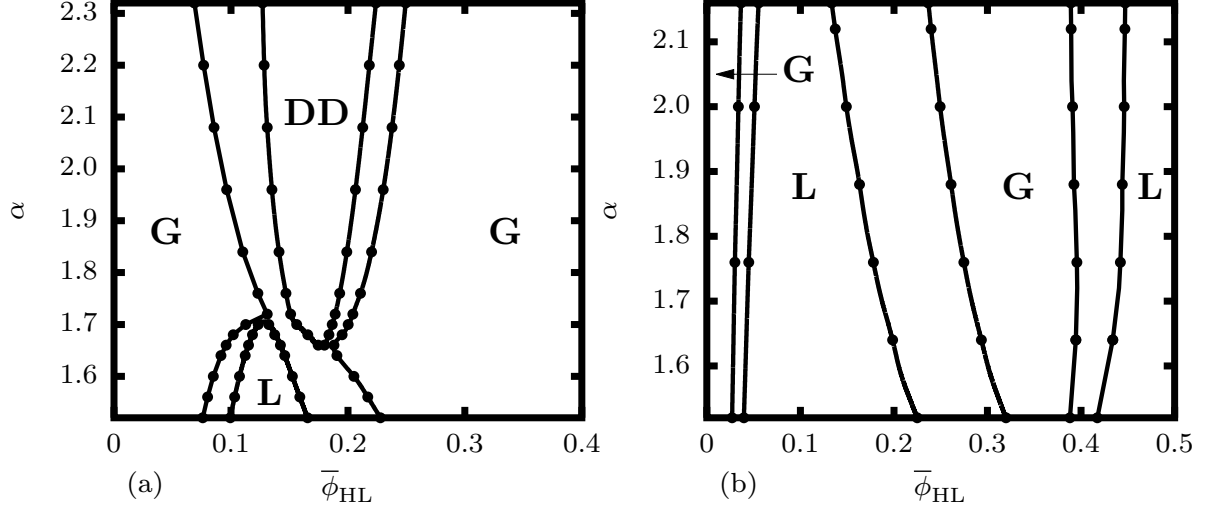


Figure 2: Phase diagrams of the binary mixture with $\chi N_G = 25$ and $f_{A,HL} = 0.95$ in the $\bar{\phi}_{HL}$ - α plane. The A-volume fraction of the G-forming copolymers is set to $f_{A,G} = 0.34$ in (a) and $f_{A,G} = 0.35$ in (b). The labels, L, G, and DD, correspond to the lamellar, double gyroid, and double diamond phases, respectively.

diblock copolymers with $f_{A,G} = 0.34$ and $f_{A,G} = 0.35$. By design, the equilibrium structure is the double gyroid phase for both diblock copolymers in the absence of the homopolymer-like additives ($\bar{\phi}_{HL} = 0$). It is interesting and surprising that the phase behaviours of these two seemingly similar diblock copolymers deviate significantly from each other when homopolymer-like additives are introduced. In the case of $f_{A,G} = 0.34$ (Figure 2 (a)), the lamellar phase emerges for $\alpha \leq 1.65$ and the DD phase appears for $\alpha \geq 1.7$ as $\bar{\phi}_{HL}$ is increased from 0. At larger $\bar{\phi}_{HL}$, a re-entrant transition to the gyroid phase occurs, similar to the case of $f_{A,G} = 0.33$ shown in Figure 1. The phase behaviour changes drastically when $f_{A,G}$ is increased slightly to $f_{A,G} = 0.35$. As shown in Figure 2 (b), in this case the intervening DD phase is replaced by the lamellae, resulting in a phase sequence of $G \leftrightarrow L \leftrightarrow G \leftrightarrow L$ when $\bar{\phi}_{HL}$ is increased. The phase diagrams shown in Figures 1 and 2 demonstrate clearly that the composition of the G-forming diblock copolymers has a drastic effect on the relative stability of the bicontinuous phases, in agreement with the result observed in the H+DBCP blends^{25–28}.

We next compare the phase behaviours of binary blends of gyroid-forming diblock copolymers mixed with homopolymers or homopolymer-like diblock copolymers. Figure 3 presents the phase

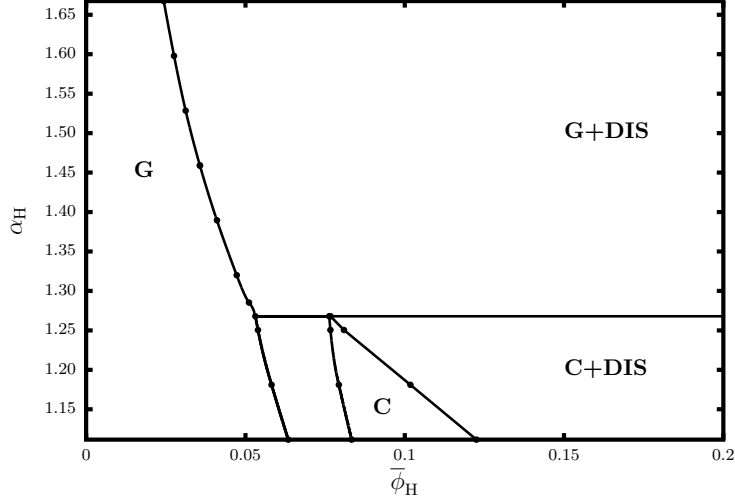


Figure 3: Phase diagram of the binary blend consisting of A-homopolymers and G-forming diblock copolymers in the $\bar{\phi}_H$ - α_H plane, with $f_{A,G} = 0.33$ and $\chi N_G = 25$. The labels, DIS, C, and G, correspond to the disordered, hexagonal, and double gyroid phases, respectively.

diagram of for the diblock copolymer/homopolymer blends as a function of the homopolymer concentration $\bar{\phi}_H$ and the homopolymer-diblock copolymer length ratio $\alpha_H = N_H/N_G$, with $f_{A,G} = 0.33$, and $\chi N_G = 25$. In order to compare with the results for the binary AB/AB blends, we focus on the th case of $\alpha_H > 1$. It is noted that G-forming diblock copolymers mixed with shorter homopolymers have been extensively studied by Matsen^{24,33} and by the Escobedo group^{25–28}. Figure 3 shows that the phase behaviour of the binary AB/A blend with longer homopolymers is relatively simple. As the homopolymer concentration increases, the parent double gyroid phase transforms to the hexagonally-packed cylinders, which persists until macrophase separation occurs between the cylindrical phase and the homopolymer-rich disordered phase when $\alpha_H < 1.25$. Above $\alpha_H = 1.25$, only the double gyroid phase is predicted to occur before the blend becomes saturated with homopolymers. We find that the value of $\bar{\phi}_H$ where macrophase separation occurs decreases with increasing α_H , which is consistent with the fact that the homopolymer solubility decreases when the homopolymers become longer. The absence of the DD phase could be attributed to the low solubility of the longer homopolymers, *i.e.* the blend becomes saturated before reaching the amount of homopolymers required to sufficiently relieve the packing frustration thus to stabilize the double diamond phase. It is clear from comparing Figures 1, and 3 that the 5% replacement of

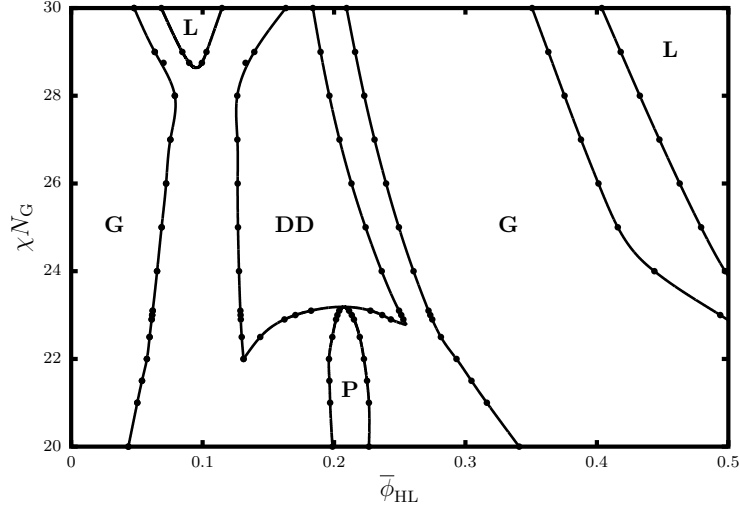


Figure 4: Phase diagram of the binary mixture with $\alpha = 2.32$, $f_{A,G} = 0.34$, and $f_{A,HL} = 0.95$ in the $\bar{\phi}_{HL}$ - χN_G plane. The labels, L, G, DD, and P correspond to the lamellar, double gyroid, double diamond, and plumber's nightmare phases, respectively.

A-monomers with B-monomers in the additives greatly improves its solubility in the blends.

We now turn to the effect of the segregation strength on the relative stability of the bicontinuous phases. Figure 4 presents the phase diagram in the $\bar{\phi}_{HL}$ - χN_G plane with $f_{A,G} = 0.34$ and $\alpha = 2.32$. These values of the parameters are chosen to yield the largest range of blend compositions where the DD phase could be accessed. As $\bar{\phi}_{HL}$ is varied, a phase transition sequence of $G \rightarrow DD \rightarrow G$ is again predicted. It is interesting to observe that decreasing the segregation strength starting from $\chi N_G = 30$ improves the stability of the DD phase by widening its region of stability. Below $\chi N_G = 23$, a third bicontinuous phase, namely the P phase, is predicted to appear. This result demonstrates that all three bicontinuous structures, *i.e.*, the G, DD and P phases, could be accessed by using the homopolymer-like diblock copolymers as additives. Furthermore, compared with diblock copolymer/homopolymer blends, the solubility of the homopolymer-like copolymers in the blends is greatly enhanced, resulting in a wider range of blend compositions where the emergence of the DD or P phases is possible.

To some extent, the improved stability of the DD phase and emergence of the P phase at lower segregation strengths could have been anticipated. It has been shown that the variations in the mean curvature on the AB interface is greatest for the P phase, and decreases as one proceeds

$P \rightarrow DD \rightarrow G$ ¹⁴. Deviations from constant mean curvature leads to excessive interfacial surface area, which is enthalpically penalized. By decreasing the segregation strength, the enthalpic cost for excessive surface area is reduced. In turn, the stability of the bicontinuous phases should improve, with improvements being greater for structures having more excessive interfacial area. This makes it more likely for the formation of the P phase to occur, provided the accompanying entropic gain outweighs the enthalpic penalty.

Mechanisms responsible for the formation of the DD and P phases in the current AB/AB blends are related to the roles played by the additives. It is useful to start by reviewing why the DD and P phases appear in H+DBCP blends. As mentioned earlier, a bicontinuous structure with constant mean-curvature will necessarily lead to a difference in thickness or size between the nodes and the struts. This gives rise to packing frustration since polymers have to stretch excessively to occupy the space at the center of the nodes that is entropically unfavourable, or else deform the nodes that is enthalpically unfavourable. Packing frustration could be alleviated through the addition of homopolymers. The added homopolymers will aggregate in the nodes, as opposed to the struts, in order to maximize its conformational entropy within the network domain²⁸. In turn, this localization of homopolymers eliminates the need for diblock copolymers to overly stretch, thus reducing packing frustration. Therefore, as the additive concentration increases, the system proceeds to bicontinuous structures with larger nodes, *i.e.* $G \rightarrow DD \rightarrow P$, in order to accommodate more homopolymers at the nodes.

We can further explore these ideas by examining the spatial distribution of the homopolymer-like copolymers within the self-assembled structures. In Figure 5, the additive volume fraction $\phi_{HL}(\mathbf{r})$ is plotted as a function of the distance from the center of a node and from the center of a strut halfway between two nodes for a typical equilibrium P phase. Figure. 5 shows that the concentration of the homopolymer-like copolymers is nearly unity near the center of the node. As one moves outwards, and approaches the AB interface, defined customarily as the $\phi_A(\mathbf{r}) = 0.5$ -isosurface, the homopolymer-like copolymer concentration rapidly decreases to zero. The behaviour at the struts is similar in that $\phi_{HL}(\mathbf{r})$ decays to zero when moving radially outwards

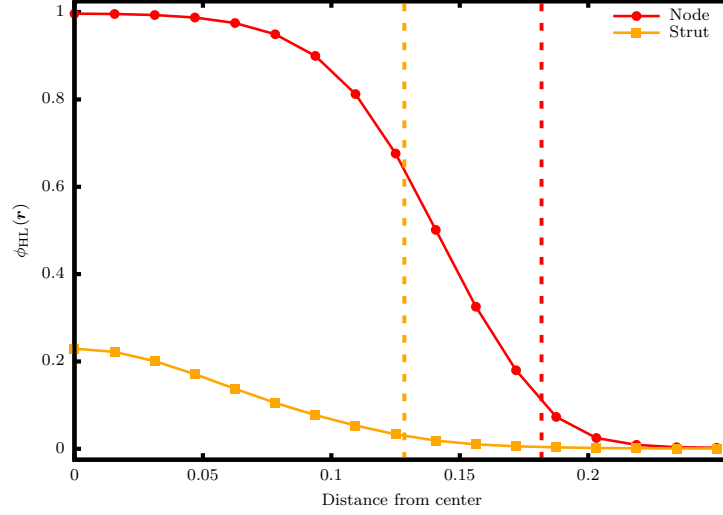


Figure 5: Plots of the volume fraction of homopolymer-like copolymers $\phi_{HL}(\mathbf{r})$ as functions of the distance from the center of a node in the [111] direction, and the distance from the center of a strut in the [100] direction for an equilibrium P phase. The data was taken from an SCFT calculation with $\bar{\phi}_{HL} = 0.2$, $f_{A,HL} = 0.95$, $f_{A,G} = 0.34$, $\chi N_G = 22.5$, and $\alpha = 2.32$. Distances have been rescaled by the length of the unit cell. The dashed lines indicate the positions of the AB interface.

from the center. However, the key difference is that the additive concentration near the center of the struts is much lower than that near the center of the nodes. This indicates that the homopolymer-like copolymers are primarily confined to the nodes within the A-domain. The results shown in Figure. 5 clearly demonstrate that the homopolymer-like diblock copolymers are localized at the center of the nodes, thus acting as space-fillers in the same way as the homopolymers would behave in H+DBCP blends, and relieving the packing frustration that hinders the stability of the DD and P phases.

The spatial distribution of the homopolymer-like copolymers depends on their concentration, $\bar{\phi}_{HL}$, in the system. Figure 6 presents $\phi_{HL}(\mathbf{r})$ as a function of the distance away from the center of a node and from the center of a strut for three values of $\bar{\phi}_{HL} = 0.2, 0.3$, and 0.4 . We note that the equilibrium structures at $\bar{\phi}_{HL} = 0.2, 0.3$, and 0.4 are P, P+G, G phases, respectively. Figure 6 (a) shows that while the AB interface moves slightly further away from the center when $\bar{\phi}_{HL}$ is increased, the behaviour of $\phi_{HL}(\mathbf{r})$ is qualitatively the same for all three blend compositions. In particular, the central region of the nodes is almost saturated with the homopolymer-like copolymers. On the other hand, the distribution of homopolymer-like copolymers in the struts behaves quite differently

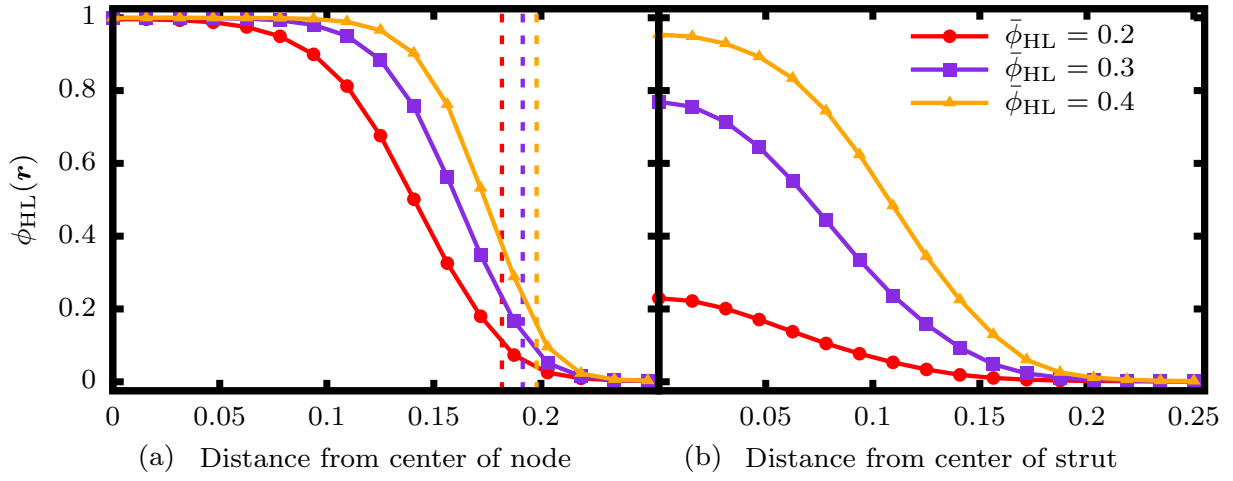


Figure 6: Plots of the volume fraction of homopolymer-like copolymers $\phi_{HL}(r)$ as functions of (a) the distance from the center of a node in the [111] direction, and (b) the distance from the center of a strut in the [100] direction for various values of $\bar{\phi}_{HL}$. The data was taken from SCFT calculations of the P phase with $f_{A,HL} = 0.95$, $f_{A,G} = 0.34$, $\chi N_G = 22.5$, and $\alpha = 2.32$. The dashed lines indicate the positions of the AB interface. Distances have been rescaled by the length of the unit cell.

as shown in Figure 6 (b). In particular, the concentration of the homopolymer-like copolymers at the center of the struts is quite low at small $\bar{\phi}_{HL} = 0.2$, and it rapidly increases to a high value when $\bar{\phi}_{HL}$ is increased. At $\bar{\phi}_{HL} = 0.4$, the concentration of the homopolymer-like copolymers almost reaches 100% at the center of the struts. At this point, the additive homopolymer-like copolymers are localized at the center of the nodes *and* the struts, *i.e.*, they are dispersed almost uniformly throughout the network domain. The accumulation of the homopolymer-like copolymers in the struts could be the origin of the subsequent transitions from bicontinuous structures with more struts per node to ones with less struts per node, *i.e.* $P \rightarrow DD \rightarrow G$. Homopolymer-like copolymers residing in the thinner nodes will experience greater confinement than those located in the nodes, which leads to a loss in conformational entropy. By returning to bicontinuous phases with less struts per node, the size of the nodes, and the struts can be made more similar. This should allow homopolymer-like copolymers both within the struts, and nodes to better maximize their conformational entropy within the A-domain.

To better understand the enhanced stability of the bicontinuous phases in the binary blends,

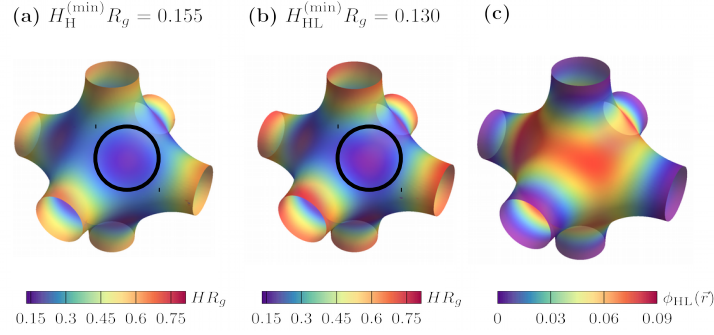


Figure 7: Plots depicting the mean curvature H of the AB-interfacial surface ($\phi_A(\mathbf{r}) = 0.5$) for (a) $\bar{\phi}_H \simeq 0.16$, and (b) $\bar{\phi}_{HL} \simeq 0.16$ with $f_{A,HL} = 0.95$, $f_{A,G} = 0.34$, $\chi N_G = 25$, and $\alpha = 2.32$. In (c), the volume fraction of the homopolymer-like copolymers $\phi_{HL}(\mathbf{r})$ on the AB interface is shown for the same P phase in (b).

we compare the mean curvature H of the AB interface for the P phase in binary blends of diblock copolymer/homopolymer with $\bar{\phi}_H = 0.16$ (Fig. 7(a)) and diblock copolymer/homopolymer-like with $\bar{\phi}_{HL} = 0.16$ (Fig. 7(b)). It is known that the packing of the different blocks with different sizes tends to curve the AB interface towards the minority domain in monodispersed diblock copolymers^{17,37}. For the bicontinuous phases, the regions of lowest interface curvature are curved towards the majority B domain, and is therefore entropically unfavourable for the G-forming DBCPs. The segregation of the homopolymer-like DBCPs to the low curvature areas relieves this curvature frustration, resulting in flatter interfaces. This effect is clearly demonstrated by the difference in the minimum value of average curvature H between the cases with homopolymer-like and homopolymer additives shown in Figures. 7(a) and (b). Moreover, the difference in the interfacial curvature between the homopolymers and homopolymer-like copolymers is correlated with the local segregation of the two polymers on the interface as shown in Fig. 7(c), where the concentration $\phi_{HL}(\mathbf{r})$ of the homopolymer-like DBCPs on the AB interface is plotted. It is clear that the distribution of the additive copolymers is not spatially uniform in that the two types of polymers are locally segregated on the interface. Furthermore, the regions where the additive concentration is the highest coincides with the regions with lowered curvature. The enhanced stability of the various bicontinuous phases in the binary blends containing homopolymer-like DBCPs could be attributed to the local regulation of the AB interfaces, *i.e.* the flattening of the interface regions at

the nodes. As a result of these two types of homopolymer-like DBCP segregations, *viz.* segregation to the center of the nodes and local segregation on the AB interfaces, the homopolymer-like DBCP functions as a “space filler” to relieve the packing frustration *and* as “co-surfactant” to regulate the interfacial curvature. These two mechanisms act in tandem resulting in greatly enhanced stability of the different bicontinuous phases.

Conclusion

We have examined the formation of various bicontinuous phases in binary mixtures of AB/AB diblock copolymers using the self-consistent field theory. We focused on the binary blends composed of gyroid-forming AB diblock copolymers with $f_{A,G} = 0.33$ to 0.35 mixed with a homopolymer-like AB diblock copolymer with $f_{A,HL} = 0.95$. Phase diagrams of the system have been constructed based on SCFT calculations. The results demonstrated that the double-diamond and plumber’s nightmare phases, which are metastable in neat diblock copolymer melts, could be stabilized by adding the homopolymer-like diblock copolymers. Furthermore, the range of blend compositions over which the DD and P phases could be accessed is larger than that of the binary H+DBCP blends. When the homopolymer-like copolymers are replaced by homopolymers, the resultant binary AB/A blends do not exhibit the DD and P phases when the homopolymer is longer than the diblock copolymer. This suggests that the 5% replacement of the A monomers with B monomers in the homopolymer plays an essential role in stabilizing the DD and P phases. By examining the spatial distribution of the different polymeric species within the self-assembled structures, we find that the homopolymer-like copolymers are confined primarily to the nodes, which alleviates the packing frustration. We also find that there is a local segregation of the two types of polymers on the AB interface, which results in beneficial changes in the interfacial curvature, further enhancing the stability of the bicontinuous phases. In the current study, we have focused on the effects of the polymer-length ratio, the segregation strength, and the composition of the G-forming diblock copolymers on the formation of novel bicontinuous phases. It is expected that tuning the

molecular composition of the homopolymer-like additive and, more interestingly, using disperse diblock copolymers with designed dispersity distributions, could provide opportunities to further improve the stability of the DD, or P phases, or perhaps even to stabilize other exotic bicontinuous structures such as the Neovious phase³⁸.

Acknowledgments

This research was supported by a Discovery Grant from the Natural Science and Engineering Research Council (NSERC) of Canada and was enabled in part by support provided by the facilities of SHARCNET (<https://www.sharcnet.ca>) and Compute Canada (<http://www.computecanada.ca>).

References

- (1) Hamley, I. *The Physics of Block Copolymers*; Oxford Science Publications; Oxford University Press, 1998.
- (2) Li, W.; Duan, C.; Shi, A.-C. Nonclassical Spherical Packing Phases Self-Assembled from AB-Type Block Copolymers. *ACS Macro Letters* **2017**, *6*, 1257–1262.
- (3) Uehara, H.; Yoshida, T.; Kakiage, M.; Yamanobe, T.; Komoto, T.; Nomura, K.; Nakajima, K.; Matsuda, M. Nanoporous Polyethylene Film Prepared from Bicontinuous Crystalline/Amorphous Structure of Block Copolymer Precursor. *Macromolecules* **2006**, *39*, 3971–3974.
- (4) Hsueh, H. Y.; Chen, H. Y.; She, M. S.; Chen, C. K.; Ho, R. M.; Gwo, S.; Hasegawa, H.; Thomas, E. L. Inorganic Gyroid with Exceptionally Low Refractive Index from Block Copolymer Templating. *Nano Letters* **2010**, *10*, 4994–5000.
- (5) Cho, B.-K.; Jain, A.; Gruner, S. M.; Wiesner, U. Mesophase Structure-Mechanical and Ionic Transport Correlations in Extended Amphiphilic Dendrons. *Science* **2004**, *305*, 1598–1601.

- (6) Crossland, E. J. W.; Kamperman, M.; Nedelcu, M.; Ducati, C.; Wiesner, U.; Smilgies, D. M.; Toombes, G. E. S.; Hillmyer, M. A.; Ludwigs, S.; Steiner, U. et al. A Bicontinuous Double Gyroid Hybrid Solar Cell. *Nano Letters* **2009**, *9*, 2807–2812.
- (7) Urbas, A. M.; Maldovan, M.; DeRege, P.; Thomas, E. L. Bicontinuous Cubic Block Copolymer Photonic Crystals. *Advanced Materials* **2002**, *14*, 1850–1853.
- (8) Alward, D. B.; Kinning, D. J.; Thomas, E. L.; Fetters, L. J. Effect of Arm Number and Arm Molecular Weight on the Solid-State Morphology of Poly(styrene-isoprene) Star Block Copolymers. *Macromolecules* **1986**, *19*, 215–224.
- (9) Thomas, E. L.; Alward, D. B.; Kinning, D. J.; Martin, D. C.; Handlin Jr, D. L.; Fetters, L. J. Ordered Bicontinuous Double-Diamond Structure of Star Block Copolymers: A New Equilibrium Microdomain Morphology. *Macromolecules* **1986**, *19*, 2197–2202.
- (10) Hasegawa, H.; Tanaka, H.; Yamasaki, K.; Hashimoto, T. Bicontinuous Microdomain Morphology of Block Copolymers. 1. Tetrapod-network Structure of Polystyrene-Polyisoprene Diblock Polymers. *Macromolecules* **1987**, *20*, 1651–1662.
- (11) Hajduk, D. A.; Harper, P. E.; Gruner, S. M.; Honeker, C. C.; Kim, G.; Thomas, E. L.; Fetters, L. J. The Gyroid: A New Equilibrium Morphology in Weakly Segregated Diblock Copolymers. *Macromolecules* **1994**, *27*, 4063–4075.
- (12) Hajduk, D. A.; Harper, P. E.; Gruner, S. M.; Honeker, C. C.; Thomas, E. L.; Fetters, L. J. A Reevaluation of Bicontinuous Cubic Phases in Starblock Copolymers. *Macromolecules* **1995**, *28*, 2570–2573.
- (13) Schulz, M. F.; Bates, F. S.; Almdal, K.; Mortensen, K. Epitaxial Relationship for Hexagonal-to-Cubic Phase Transition in a Block Copolymer Mixture. *Physical Review Letters* **1994**, *73*, 86.

- (14) Matsen, M. W.; Schick, M. Stable and Unstable Phases of a Diblock Copolymer Melt. *Physical Review Letters* **1994**, *72*, 2660–2663.
- (15) Meuler, A. J.; Hillmyer, M. A.; Bates, F. S. Ordered Network Mesosstructures in Block Polymer Materials. *Macromolecules* **2009**, *42*, 7221–7250.
- (16) Matsen, M. W.; Bates, F. S. Origins of Complex Self-Assembly in Block Copolymers. *Macromolecules* **1996**, *29*, 7641–7644.
- (17) Matsen, M. W. The standard Gaussian model for block copolymer melts. *Journal Of Physics-Condensed Matter* **2002**, *14*, R21–R47.
- (18) Hasegawa, H.; Hashimoto, T.; Hyde, S. T. Microdomain Structures with Hyperbolic Interfaces in Block and Graft Copolymer Systems. *Polymer* **1996**, *37*, 3825–3833.
- (19) Sides, S. W.; Fredrickson, G. H. Continuous Polydispersity in a Self-Consistent Field Theory for Diblock Copolymers. *The Journal of Chemical Physics* **2004**, *121*, 4974–4986.
- (20) Cooke, D. M.; Shi, A.-C. Effects of Polydispersity on Phase Behavior of Diblock Copolymers. *Macromolecules* **2006**, *39*, 6661–6671.
- (21) Matsen, M. W. Polydispersity-induced macrophase separation in diblock copolymer melts. *Physical Review Letters* **2007**, *99*, 148304.
- (22) Lynd, N. A.; Meuler, A. J.; Hillmyer, M. A. Polydispersity and block copolymer self-assembly. *Progress In Polymer Science* **2008**, *33*, 875–893.
- (23) Liu, M.; Qiang, Y.; Li, W.; Qiu, F.; Shi, A.-C. Stabilizing the Frank-Kasper Phases via Binary Blends of AB Diblock Copolymers. *Acs Macro Letters* **2016**,
- (24) Matsen, M. W. Stabilizing New Morphologies by Blending Homopolymer with Block Copolymer. *Physical Review Letters* **1995**, *74*, 4225–4228.

- (25) Martínez-Veracoechea, F. J.; Escobedo, F. A. Monte Carlo Study of the Stabilization of Complex Bicontinuous Phases in Diblock Copolymer Systems. *Macromolecules* **2007**, *40*, 7354–7365.
- (26) Martínez-Veracoechea, F. J.; Escobedo, F. A. Bicontinuous Phases in Diblock Copolymer/Homopolymer Blends: Simulation and Self-Consistent Field Theory. *Macromolecules* **2009**, *42*, 1775–1784.
- (27) Martínez-Veracoechea, F. J.; Escobedo, F. A. The Plumber’s Nightmare Phase in Diblock Copolymer/Homopolymer Blends. A Self-Consistent Field Theory Study. *Macromolecules* **2009**, *42*, 9058–9062.
- (28) Padmanabhan, P.; Martínez-Veracoechea, F. J.; Escobedo, F. A. Computation of Free Energies of Cubic Bicontinuous Phases for Blends of Diblock Copolymer and Selective Homopolymer. *Macromolecules* **2016**, *49*, 5232–5243.
- (29) Takagi, H.; Yamamoto, K.; Okamoto, S. Ordered-Bicontinuous-Double-Diamond Structure in Block Copolymer/Homopolymer Blends. *Europhysics Letters* **2015**, *110*, 48003.
- (30) Takagi, W.; Suzuki, J.; Aoyama, Y.; Mihira, T.; Takano, A.; Matsushita, Y. Bicontinuous Double-Diamond Structures Formed in Ternary Blends of AB Diblock Copolymers with Block Chains of Different Lengths. *Macromolecules* **2019**, *52*, 6633–6640.
- (31) Fredrickson, G. H. *The Equilibrium Theory of Inhomogeneous Polymers*; Oxford University Press, 2006; Vol. 134.
- (32) Shi, A.-C. *Self-consistent Field Theory of Inhomogeneous Polymeric Systems, in Variation Methods in Molecular Modeling*, J. Wu (ed.); Springer, 2017.
- (33) Matsen, M. W. Phase Behavior of Block Copolymer/Homopolymer Blends. *Macromolecules* **1995**, *28*, 5765–5773.

- (34) Thompson, R. B.; Rasmussen, K. Ø.; Lookman, T. Improved Convergence in Block Copolymer Self-Consistent Field Theory by Anderson Mixing. *Journal of Chemical Physics* **2004**, *120*, 31–34.
- (35) Tzeremes, G.; Rasmussen, K. Ø.; Lookman, T.; Saxena, A. Efficient Computation of the Structural Phase Behavior of Block Copolymers. *Physical Review E* **2002**, *65*, 041806.
- (36) Rasmussen, K. Ø.; Kalosakas, G. Improved Numerical Algorithm for Exploring Block Copolymer Mesophases. *Journal of Polymer Science Part B: Polymer Physics* **2002**, *40*, 1777–1783.
- (37) Semenov, A. N. Contribution to the Theory of Microphase Layering in Block-Copolymer Melts. *Journal of Experimental and Theoretical Physics* **1985**, *61*, 733.
- (38) Stroem, P.; Anderson, D. M. The Cubic Phase Region in the System Didodecyldimethylammonium Bromide-Water-Styrene. *Langmuir* **1992**, *8*, 691–709.

Graphical TOC Entry

Various bicontinuous phases are stabilized
in diblock copolymer blends

